# Omniphobic etched aluminum surfaces with anti-icing ability

*Marta Fenero[1], Mato Knez[2,3], Iva Saric[4], Mladen Petravic[4], Hans Grande[1], Jesús Palenzuela[*1]*

[1]CIDETEC, Basque Research and Technology Alliance (BRTA), Po. Miramón 196, 20014 Donostia-San Sebastián, Spain

[2]CIC nanoGUNE BRTA, Tolosa Hiribidea, 76, 20018 Donostia - San Sebastián, Spain

[3]Ikerbasque, Basque Foundation for Science, María Díaz de Haro 3, 48013 Bilbao, Spain

[4]University of Rijeka, Department of Physics and Center for Micro- and Nanosciences and Technologies, R. Matejcic 2, 51000 Rijeka, Croatia

KEYWORDS: anti-icing, freezing delay time, ice formation, omniphobicity, chemical etching, aluminum, perfluoropolyether

ABSTRACT In this work, omniphobic surfaces are developed by combining chemical etching and surface modification of aluminum. In the first step, a hierarchical micro/nanostructuring is carried out by chemical etching. Thereafter, a perfluoropolyether is grafted onto the corrugated aluminum substrate, decreasing its surface free energy and turning the system omniphobic. The morphology and chemical composition of the developed surfaces are characterized. We observed

a low affinity towards liquids, regardless of their chemical nature and surface tension. The surface shows superhydrophobic properties with water contact angles of 160° and simultaneously strong oleophobic properties with hexadecane contact angles of 141°. Furthermore, these omniphobic surfaces significantly delay the freezing time of water droplets to 5100 seconds, which is about 20-fold of the freezing time on pristine aluminum (260 seconds) and they even inhibit ice growth by repelling the incoming droplets prior to ice nucleation.

## INTRODUCTION

The wetting properties of surfaces play an enormous role in numerous applications. Repellent surfaces are either hydrophobic or oleophobic and are usually designed to repel either polar or nonpolar liquids. However, those properties are not mutually exclusive. Omniphobic surfaces offer the potential to repel both high and low surface tension liquids, including water, oils and alcohols.[1,2] Designing omniphobic surfaces has attracted interest in recent years due to their broad impact on industrial applications, including self-cleaning,[3,4,5] anti-fouling,[6] water-oil separation[7] and anti-icing,[8,9,10]

The impact of the surface on safety risks and the economy is huge. According to the United States National Highway Traffic Safety Administration (NHTS) data, approximately 21% of vehicle crashes are related to weather conditions and average statistics show that annually more than 150,000 crashes occur because of icy roads.[11] Electrical power lines often suffer failures due to excessive ice loading[12] and ice accumulated on wings of aircrafts negatively or even catastrophically affects the aerodynamic performance disrupting laminar airflows and decreasing the lift force.[13] Additionally, icing of wind turbine blades can reduce the annual wind energy conversion by 50%.[14] Functionalizing surfaces to prevent icing (anti-icing) and to repel

ice (ice-phobic) became greatly interesting for both fundamental research and industrial applications.

The low surface free energy (SFE) of omniphobic surfaces may benefit anti-icing behavior by delaying the freezing time of water droplets and/or repelling water droplets from the surface before freezing starts. The use of perfluorinated compounds is widely proposed to obtain such low SFE surfaces. However, this family of compounds has been identified to cause a number of environmental issues.[15] Indeed, the use of perfluorinated molecules with chains longer than eight carbon atoms has been limited for several applications due to their toxicity, high persistence and bioaccumulation.[16] Therefore, to achieve persistent liquid repellency for various applications, omniphobic surfaces, based on alternative low SFE compounds, are sought for.[16]

Omniphobic surfaces with covalently anchored perfluoropolyethers (PFPEs), able to repel any type of liquids, including water droplets, appear to be excellent candidates to address the above-mentioned issues.[17] Indeed, the use of PFPEs has been investigated after anchoring to smooth surfaces[18,19] or forming hybrid sol-gel coatings.[20,21] However, a direct covalent anchoring of PFPE molecules on tailor-made nanostructured surfaces is still unexplored.

In this paper, a simple method to develop omniphobic aluminum surfaces with anti-icing properties by combining chemical etching and surface modification is reported. Aluminum has been selected as a base material for this development because of its relevance for the current and future industrial products. Its low specific weight, excellent thermal and electrical conductivity and low cost made it one of the most used metals in materials engineering. A hierarchical micro/nanostructuring of the aluminum surface was carried out through chemical etching with ferric chloride. Subsequently, the surface was modified with

perfluoro(polypropyleneoxy)methoxypropyltrimethoxysilane, an environmentally safe and non-toxic low SFE compound, in order to add omniphobic properties to the system. The wetting behavior of the developed surfaces and their relation to their surface roughness and chemical composition is discussed. The obtained omniphobic surfaces are tested against different liquids in order to characterize their omniphobicity. More importantly, we show for the first time that a PFPE, directly attached to the substrate, provides anti-icing properties. The freezing delay of water droplets and the ice formation process are analyzed to assess the anti-icing performance.

## EXPERIMENTAL SECTION

### Materials

The used substrate was a 1050 aluminum alloy (provided by Alu stock) with a chemical composition of Al: 99.08 % min, Mg: ≤ 0.05 %, Mn: ≤ 0.05 %, Fe: ≤ 0.40 %, Si: ≤ 0.25 %, Cu: ≤ 0.05 %, Zn: ≤ 0.07 %, Ti: ≤ 0.05 %. Ferric chloride hexahydrate (98%) and hexadecane (98%) were purchased from Sigma-Aldrich. Hydrochloric acid (37%), ethanol (96%) and acetone (96%) were purchased from Scharlab. Perfluoro(polypropyleneoxy)methoxypropyltrimethoxysilane (PFPE, 20% in fluorinated hydrocarbon) was purchased from Gelest. Perfluorotripentylamine (FC-70, 85%) was acquired from Apollo Scientific. Millipore water with a conductivity of 0.054 μS/cm was used in all experiments. All reagents were used as received.

### Methods

#### *Fabrication of hierarchical micro/nanostructuring on aluminum surfaces by chemical etching*

Before the chemical etching, the aluminum substrates were washed with soap and thoroughly rinsed with millipore water, followed by sonication in acetone, ethanol and deionized water for 10 minutes each at room temperature. Subsequently, chemical etching of the cleaned substrates was performed by immersion into a 14 wt. % aqueous ferric chloride solution at 50 °C for various periods of time.[22] After etching, the samples were cleaned by sonication in isopropyl alcohol for 10 minutes and dried in a nitrogen gas stream.

***Chemical modification of aluminum surfaces***

Functionalization of pristine substrates and etched aluminum samples with PFPE was performed by drop-casting a 0.1 wt. % PFPE dispersion in FC-70. Special care has been taken that the surface of the sample was completely covered by the dispersion. After that, samples were stored in an oven with saturated humidity conditions at 60 °C during 3 hours to promote the hydrolysis of the PFPE molecules. Finally, an additional thermal treatment at 100 °C was carried out for 3 hours.

***Surface characterization***

The surface morphology of the samples was analyzed using an ULTRA plus ZEISS field emission scanning electron microscope (FESEM). The examinations were carried out at 7 kV accelerating voltage. Topographical surface images were captured using a Leica DCM 3D confocal microscope. The surface roughness of the samples was examined using a Talysur 50 mm Intra Taylor Hobson profilometer. The average of the surface roughness values was obtained by measuring at ten different positions.

Fourier transform infrared spectra (FTIR) of the samples were obtained with a PerkinElmer Frontier spectrometer equipped with an ATR sampling stage. The spectra were acquired from 20 scans from 800 $cm^{-1}$ to 4000 $cm^{-1}$ and a resolution of 4 $cm^{-1}$.

The surface composition of pristine and treated surfaces was analyzed by X-ray photoelectron spectroscopy (XPS). The experiments were performed using a SPECS instrument equipped with a hemispherical electron analyzer and a monochromatized source of Al $K_\alpha$ X-rays. The calibration of the energy scale in all spectra was done by positioning the binding energy of the characteristic C 1*s* peak at 284.5 eV. The XPS spectra were deconvoluted into several sets of mixed Gaussian-Lorentzian (G-L) functions with Shirley background subtraction.[23]

An Attension Theta Lite optical tensiometer was used to determine the contact angles of the films. Droplets of solvents were placed on a minimum of three different areas of the surface. The static contact angles were recorded using the Laplace-Young fitting method. The total SFE of the coatings was determined according to the Fowkes model using water and ethylene glycol as polar liquids and diiodomethane as non-polar liquid.

The anti-icing experiments were carried out with an optical tensiometer. A fluid circulating cooling stage and the measuring chamber accessories were coupled to the equipment for temperature control and environmental protection, respectively. To determine the *freezing delay time*, the cooling stage temperature was decreased from room temperature to -11 °C at a relative humidity about 30% and the sample was placed over it. Once this temperature was reached, the sample was preconditioned for 10 minutes. Afterward, a 5 µL droplet of deionized water was placed on the cooled aluminum surface. The time at which the water droplet started to freeze was considered as freezing delay time. To evaluate the *ice formation* and accretion process, the

substrates were fixed to the cooling stage with a tilted angle of 10° and allowed to cool down to -10 °C. A 5 µL droplet of deionized water was placed onto the aluminum surface. All the experiments were monitored through the images obtained from the high-speed camera of the optical tensiometer equipment.

The omniphobic performance of the surfaces was evaluated by testing their ability to repel methylene blue-dyed water and olive oil droplets.

## RESULTS AND DISCUSSION

### Surface morphology of the micro/nanostructured surfaces

As a first step, the etching time was optimized in order to induce superhydrophobicity by the generation of micro-nanoscale roughness on the aluminum surface. This was achieved by immersion in a ferric chloride solution as described in the Methods part. After proceeding with a systematic study by varying the immersion time and the bath temperature, the optimal experimental conditions were identified to be 20 minutes etching at 50 °C, as shown in **Figure S1**. The surface morphology of the aluminum samples was analyzed by FESEM at different magnifications (**Figure 1**). A relatively smooth surface ($R_a = 0.401 \pm 0.036$ µm and $R_z = 2.639 \pm 0.707$ µm determined by profilometer) without the presence of significant structural motifs was observed for the pristine aluminum (**Figure 1a, 1b**). In contrast, micro and nanoscaled rectangular features, uniformly distributed over the surface, were observed on the samples etched under optimal etching conditions (**Figure 1c**). At higher magnification (**Figure 1d**) the formation of iron spherulites could be observed, which increased the surface roughness

($R_a = 1.084 \pm 0.347$ µm and $R_z = 8.071 \pm 2.498$ µm) and generated a hierarchical structure, as previously reported by Maitra *et al*.[22]

In addition to FESEM micrographs, 3D topographical images (**see Figure S2**) and the roughness analysis in terms of $R_a$ and $R_z$ showed in **Table S1** confirmed the increase of surface roughness as the etching time continuously increases.

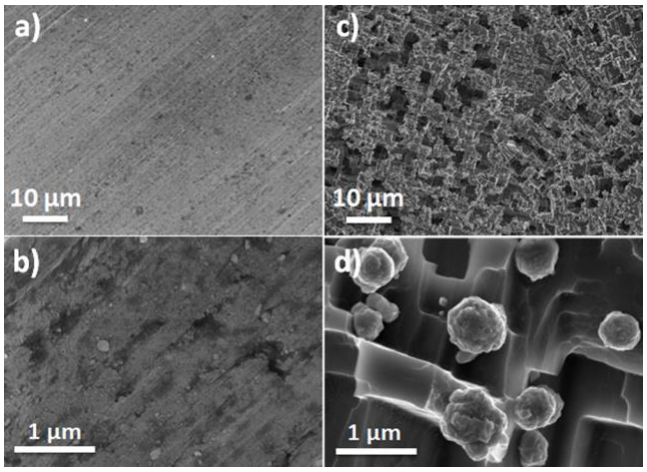


**Figure 1.** a) Low and b) high magnification FESEM micrographs of the pristine aluminum substrate. c) Low and b) high magnification FESEM micrographs of the aluminum surface after chemical etching using 14 wt. % aqueous ferric chloride solution for 20 minutes at 50 °C.

**Chemical composition of the modified surfaces**

In the next step, the corrugated surface was subjected to chemical modification with PFPE in order to reduce the SFE. The grafting of PFPE to the aluminum surface was evaluated by ATR-FTIR and XPS. ATR-FTIR spectra of a pristine aluminum substrate and a PFPE film grafted onto a rough aluminum substrate are shown in **Figure 2a.** Characteristic absorption peaks of $CF_2$ and $CF_3$ groups, corresponding to the stretching vibration of C-F bonds, were observed between 1150 $cm^{-1}$ and 1200 $cm^{-1}$.[24] The peak at 1006 $cm^{-1}$ can be assigned to the C-O-C ether bond. The

presence of these characteristic bands are in agreement with those of pure PFPE and confirm the presence of PFPE molecules on the surface of the rough aluminum substrate. Similar absorption bands were obtained for the PFPE deposited on smooth aluminum (see **Figure S3**), which confirms successful surface functionalization. However, the sloping down of the baseline observed on the rough sample indicates a difference to the smooth substrate. This sloping was attributed to the scattering of the light on the rough surface.

In addition to ATR-FTIR analysis, XPS spectroscopy was used in order to gain more insight into the surface chemical composition. The XPS survey spectra, shown in **Figure S4** of Supporting Information, reveal a significant change in surface chemical composition after functionalization of the etched aluminum surface with PFPE. The atomic concentrations obtained from spectra in Figure **S4** are listed in **Table 1**. A strong O 1s peak observed on both surfaces, reflecting the relatively high oxygen concentration as listed in **Table 1**, indicates the presence of oxidized aluminum surfaces. Indeed, the photoemission around the Al 2p core level, shown in **Figure S5a** for the unmodified surface was fitted with two mixed Gaussian-Lorentzian (G-L) functions, assigned to the metallic Al, $Al^0$, and Al oxide, $Al_2O_3$, while the modified surface exhibits an additional peak related to some Al suboxides, Al-O (see **Figure S5b**). In addition, a strong C 1s peak from the pristine aluminum surface is related mostly to the airborne hydrocarbons adsorbed on the surface as confirmed by XPS (not shown).

**Table 1**. The atomic concentrations of O, Al, C and F from unmodified aluminum substrate and PFPE film deposited onto rough aluminum substrate.

| **Sample** | **Atomic concentrations (%)** | | | |
|---|---|---|---|---|
| | O | C | F | Al |
| Unmodified aluminum substrate | 33.7 | 39.1 | 1.7 | 25.5 |

| | | | | |
|---|---|---|---|---|
| PFPE film deposited onto rough aluminum | 17.7 | 31.5 | 41.4 | 9.4 |

**Figure 2b** shows the photoemission spectra of the PFPE film grown on the etched aluminum substrate around the C 1*s* core level. The C 1*s* emission exhibits a number of components originating from different carbon bonds of different relative concentrations. Eight contributions were employed for the Gaussian-Lorentzian (G-L) deconvolution to obtain a good fit of the experimental spectra. The photoemission from the PFPE-modified surface is dominated by the set of bonds related to the C-F complexes characteristic for PFPE. We assign the three peaks (peaks 2, 3, and 4) at the binding energy (BE) of 293.3eV, 291.0 eV and 289.05 eV to the characteristic C-$F_3$, C-$F_2$ and O-$CH_2$-O bonds, respectively, in good agreement with the literature.[25,26] Peak 1, at 292.4 eV, can be assigned to the C 1*s* emission from carbon $F_2$C-O bonds,[27,28] while the feature on the lower BE side (peak 8) corresponds to the C-Si bonds.[29,28] Besides, three carbon-related components characteristic for contaminated surfaces were also detected: C-C/C-H, C-O and C=O bonds at 284.5 eV, 285.95 eV and 287.75 eV, respectively (peaks 7, 6 and 5). The major contribution of these peaks (especially peaks 5 and 7) in the spectrum obtained from smooth surfaces (that is from non-etched and, consequently, more polluted surface) (see **Figure S6**) supports the hypothesis of surface carbon contamination as the main origin of the peaks 5-7. The presence of $CF_3$, $CF_2$, $CF_2$-$CH_2$ or O-$CF_2$ bonding combinations reveals the functionalization of aluminum surfaces with fully grown PFPE films.

The O 1s photoemission, shown in **Figure S7**, confirms further the functionalization of oxidized Al surfaces, characterized by an intensive peak at the BE of 535.5 eV related to the O-$CF_2$ bonds.[30,28]

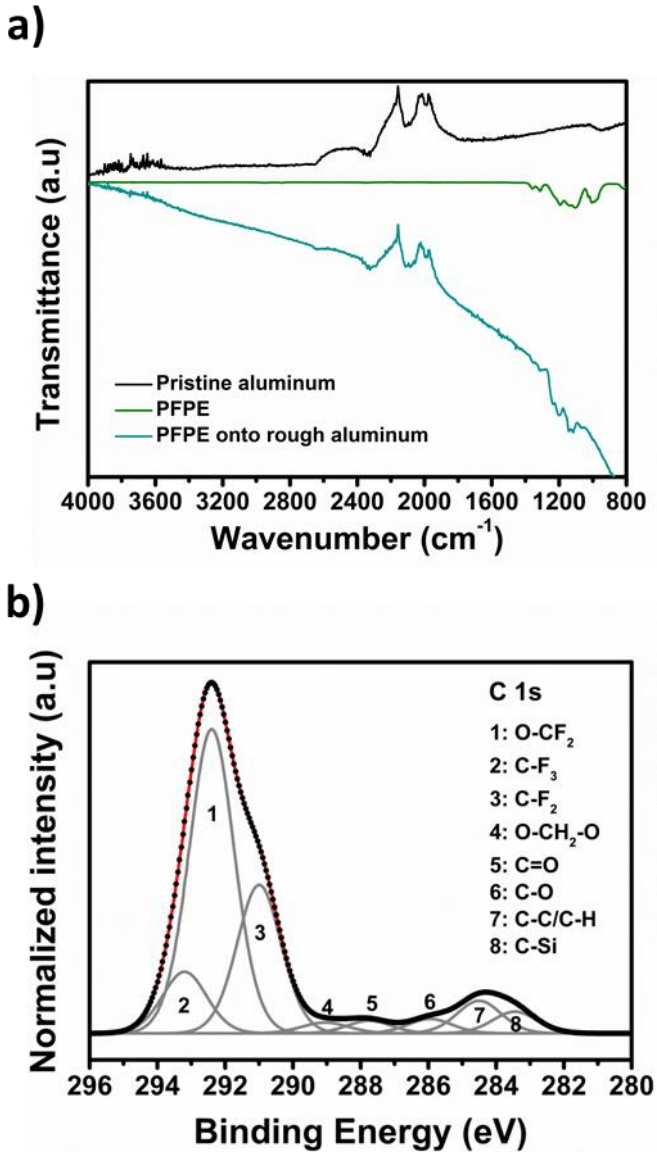


**Figure 2.** a) ATR-FTIR spectrum of an unmodified aluminum substrate (black), PFPE deposited onto a rough aluminum substrate (cyan) and pure PFPE (green). b) XPS around C 1*s* core levels of PFPE film deposited onto a rough aluminum substrate.

**Wetting behavior of the modified surfaces**

It is well known that the wettability of materials depends on both, the chemical composition, and the surface roughness. We used contact angle (CA) measurements to evaluate the effect of the PFPE grafting to aluminum substrates and the chemical etching to induce the surface roughness on the wettability. **Figure 3a** shows the results obtained using water and hexadecane as liquid probes in order to evaluate the wetting and omniphobicity of the prepared surfaces. Pristine and PFPE-modified aluminum substrates were subjected to water and oil repellency tests. As expected, the water and hexadecane CA for the pristine aluminum significantly increased after PFPE grafting from 70° to 116° and from <10° to 68°, respectively. Therefore, the wetting properties of aluminum changed from superomniphilic to omniphobic. This was attributed to the presence of $-CF_2$ and $-CF_3$ groups from the PFPE, which again confirms the surface functionalization. In addition, a strong relationship between the surface roughness and the CA was observed. The influence of the structuring of the aluminum surfaces was studied by chemical etching during different periods of time (see **Figure S1**). After PFPE grafting of the etched substrates, short etching times (1 minute) did not show any influence on the CA values. This fact is consistent with the observed surface morphology of the sample (**Figure S1 a**), which was rather smooth with only small regions with structural motifs. Increasing the etching time progressively increased the CA, reaching 160° in the case of water and 141° for hexadecane, for samples which underwent 20 minutes of etching treatment. In order to gain further insight into the liquid-solid interactions, the SFE of the various surfaces was determined. In general, the wettability of a solid by a liquid is reduced by lowering its SFE. Besides, it is important to take into account the nature of the SFE components, because they strongly affect the liquid-solid interactions.[31] According to the Fowkes model, the SFE can be defined as a sum of its polar and

dispersive components and the contribution of each of them to the total SFE determines the affinity of a surface to liquids, depending on their polar or non-polar nature.[32]

**Figure 3b** displays the SFE of the different surfaces and the contribution of their polar and non-polar components. As expected, the SFE of the pristine aluminum (39.22 mN/m) was reduced after the PFPE modification (10.80 mN/m). A further reduction was observed from etched samples, where a direct correlation between the reduction of the SFE and the increased surface roughness which was monitored in the present study by the etching time was also observed. Note the extremely low SFE of the samples etched during 20 and 30 min., reaching values as low as 1.8 mN/m and 0.3 mN/m, respectively. An important observation is that, after modification, the contribution of the polar component to the total SFE is very little and almost negligible, as can be seen in **Figure 3b**. This means that lowering the affinity of a surface to a liquid is more strongly expressed with polar liquids like, for example, water. This insight consequently suggests the potential of the developed samples as an efficient anti-icing substrate. Furthermore, the stability of the surface modification was demonstrated by measuring the water and the hexadecane CA of the samples 10 months after their preparation, showing no variation of their CA´s values.

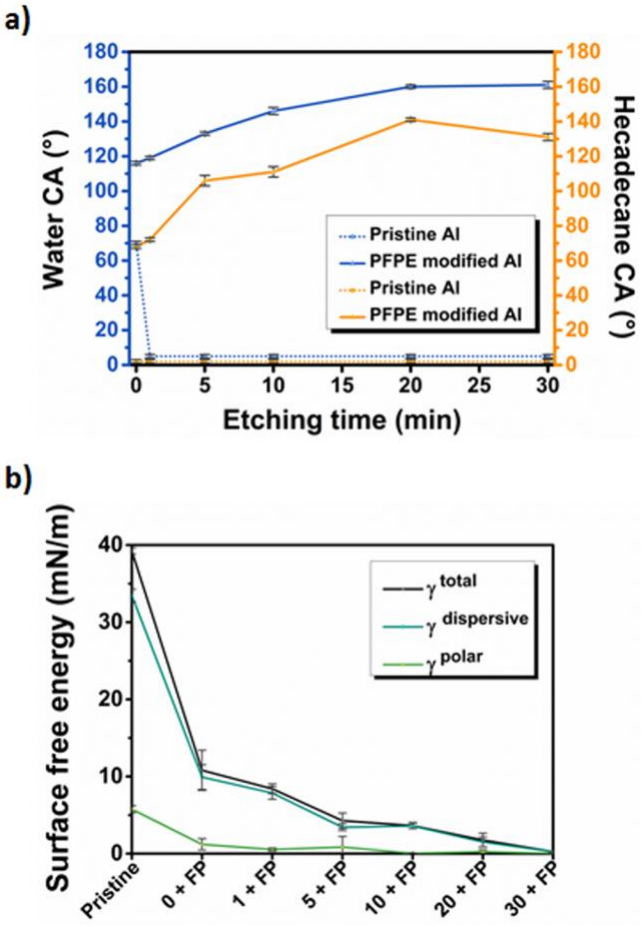


**Figure 3**. a) Static contact angles observed for pristine aluminum and PFPE-modified aluminum before and after chemical etching during different etching times. b) Total surface free energy and it's dispersive (non-polar) and polar components determined using the Fowkes model for pristine aluminum, PFPE-modified aluminum and PFPE-modified aluminum after chemical etching treatment during different etching times. The numbers x + PFPE indicate the etching times (in minutes).

**Anti-icing performance of omniphobic coatings**

The weak interaction of the surface and polar liquids, such as water, may benefit the anti-icing performance of the developed omniphobic surfaces. Therefore, the freezing delay time and the ice formation from impinging droplets were evaluated, as depicted in **Figure 4**.

The freezing delay time of water droplets was determined on both smooth and rough aluminum substrates, modified by PFPE, along with the pristine aluminum substrate, in order to evaluate the influence of the surface roughness on the freezing time. **Figure 4a** shows the evolution of a 5 μL water droplet, placed onto the three different samples, from the liquid state to the frozen state. In all three samples, the water droplet showed similar behavior. In liquid state the droplet was transparent. The start of the freezing process was identified by the reduction of the transparency of the droplet. After freezing, the shape of the droplet changed showing a tip on the top of the droplet (see **Figure S8**). It is noted that during the freezing process of a water droplet, the freezing front moved from the solid-liquid interface to the top of the droplet, exhibiting heterogeneous freezing mechanism. The time needed for the droplet to freeze was significantly different for each surface. In the case of the pristine aluminum substrate, the droplet becomes completely frozen in 260 ± 15 seconds, while on the smooth PFPE-functionalized aluminum surface it took 780 ± 60 seconds. In contrast, for the rough PFPE-modified aluminum the time until freezing of the droplet was 5100 ± 125 seconds, considerably more than with the other two samples. The significant increase in the freezing time can be related to two different effects. On the one hand, the SFE of the pristine aluminum was reduced from 39.22 mN/m to 10.80 mN/m after modification with PFPE (smooth aluminum functionalized with PFPE). This SFE reduction, together with the low contribution of the polar component to the total SFE, lowered the affinity between the water droplet and the material surface, giving rise to an increase in the freezing delay time. The time required for a water droplet to freeze on the low SFE sample was 780 ± 60

seconds, thereby 3-fold that on pristine aluminum (260 ± 15 seconds). On the other hand, surface morphology also played an important role in the increase of freezing time. With 5100 ± 125 seconds the freezing time on rough and PFPE-modified aluminum outperformed the freezing times on the other investigated surfaces. This remarkable increase of the freezing time by a factor of more than 6 was achieved by corrugation when compared to the smooth PFPE-modified. Furthermore, by combining the surface structuring and PFPE-modification an almost 20-fold delay in the freezing time compared to the pristine aluminum substrate was achieved. This behavior is attributed to the thermal conductivity. The thermal conductivity is related to the contact area between two phases, in this case, between the substrate surface and the droplet surface.[33] On smooth surfaces, the contact area is maximized, in dependence on the wettability, thus the thermal conduction is also maximized. Consequently, the droplet freezes quickly on smooth surfaces. In contrast, if the droplet is placed onto a surface with a structured morphology in the Cassie-Baxter wetting regime, air will be trapped below the water droplet, thereby minimizing the contact area between the surfaces of the substrate and water droplet. The air trapped in the surface cavities is a poor thermal conductor and together with the reduction of the contact area, will considerably hinder the heat transfer between the substrate and the liquid, significantly delaying the freezing time of the droplet.[34,35,36] The low hysteresis CA (7º) along the high CA (160º) displayed by the PFPE-modified rough aluminum reveals that the droplet on this surface is in the Cassie-Baxter wetting regime, preventing the water penetration between the surface topography features and trapped air pockets and delaying the frost formation process. Despite the heterogeneous ice nucleation theory, which establishes that a critical radius of ice nuclei smaller than the size of the surface features allows spontaneous ice growth,[37] and an ice nuclei radio of 4.5 nm calculated at -10 ºC,[38] significantly smaller than the size of the surface

features on the rough aluminum (see **Figure 1**, **Figure S2** and **Table S1**), the substantial increase on the freezing delay time observed on the PFPE-modified rough aluminum, is attributed to the surface topography and to the small solid-liquid contact area and air pockets entrapped on the hierarchical micro/nanostructuring (hindering the heat transfer) providing a low rate for ice nucleation and growth as was previously described in references [39] and [36].

Furthermore, ice formation from impacting droplets was evaluated on the three different samples as shown in **Figure 4b**. The experiment was carried out by tilting the substrates to 10° at a temperature of -10 °C and dropping one water droplet on the surface of each sample. As expected from the wettability, and according to the literature,[40] the hydrophilic nature of the pristine aluminum substrate allowed the incoming water droplet to rest in contact with the surface, in this way promoting the ice nucleation and the subsequent droplet freezing (**Figure 4b i**). On the PFPE-modified smooth aluminum (**Figure 4b ii**), despite reduced interaction, the water droplet remains in contact with the surface and the freezing process occurs in a short period of time. However, on the rough PFPE-modified aluminum (**Figure 4b iii**), the impinging droplet fully bounced off of the surface before the ice nucleation started, thus preventing the ice formation. The above results verify the significantly greater efficiency of the rough, PFPE-modified aluminum surface in the prevention of the ice formation than the pristine aluminum. Both, freezing delay time and ice formation experiments of **Figure 4** confirm the great potential of the developed omniphobic surface as an anti-icing solution.

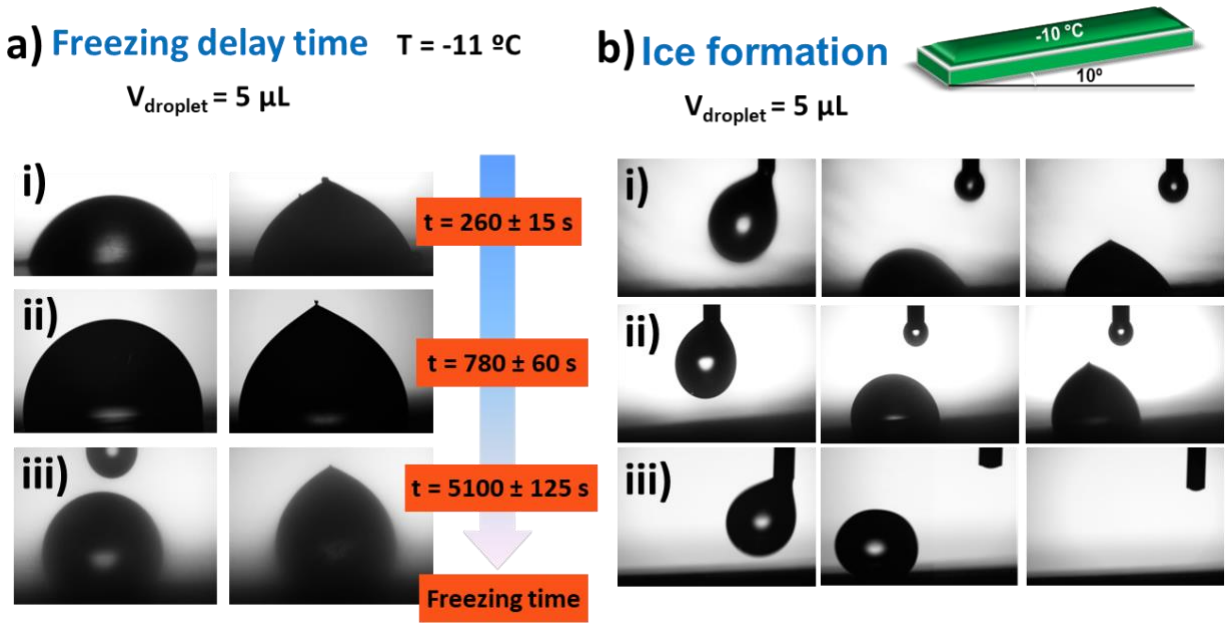


**Figure 4**. Anti-icing properties: a) Freezing delay time, b) Ice formation on i) Pristine aluminum, ii) PFPE-grafted smooth aluminum, iii) PFPE-grafted rough aluminum.

In addition to assessing the anti-icing performance of the omniphobic surfaces against impinging water droplets, the frost formation from condensed droplets was also examined. The low-temperature icing experiments were carried out on the cooling stage at -5 ºC with a RH of 60% ± 5%. As shown in **Figure 5**, condensed droplets start to appear within 10 min on the pristine aluminum, completely covering the surface in 20 min. The aluminum surface was totally covered by ice in 30 min. The same behavior was observed for the PFPE-grafted on the smooth aluminum, however, the times required for the water droplets to condensate (30 min) and completely freeze (61 min) on the surface, were significantly higher. This fact was attributed to the lower SFE (i.e. less affinity for water) of these surfaces compared to that of the pristine aluminum. In contrast, tiny condensed droplets were not observed on the PFPE-grafted rough aluminum until 30 min after beginning the essay. After 85 min, a layer of ice completely covered the surface. Note that this time is notably higher than that required by both, the pristine

aluminum (30 min) and the PFPE-grafted on rough aluminum (61 min) surfaces to freeze. This significant delay on the ice formation is attributed to its low thermal conductivity derived from the low contact area between the droplet and the surface as consequence of the trapped air pockets on its hierarchical micro/nanostructuring.[41] This result reveals that the PFPE-grafted on rough aluminum exhibits an increase on the icing delay time by almost 3-fold than on the pristine aluminum.

The durability of the anti-icing properties of the surfaces was evaluated by measuring the contact angle of the samples after 5 freeze-thaw cycles. Contact angle values similar to those in the initial samples (prior to performing the freeze-thaw essay) were obtained. In addition, the freezing delay time of a droplet on the PFPE-modified aluminium surfaces has been determined three times on the same sample, displaying a similar freezing delay time in all the essays. These results prove that the anti-icing performance is also maintained after 3 freeze-thaw cycles.

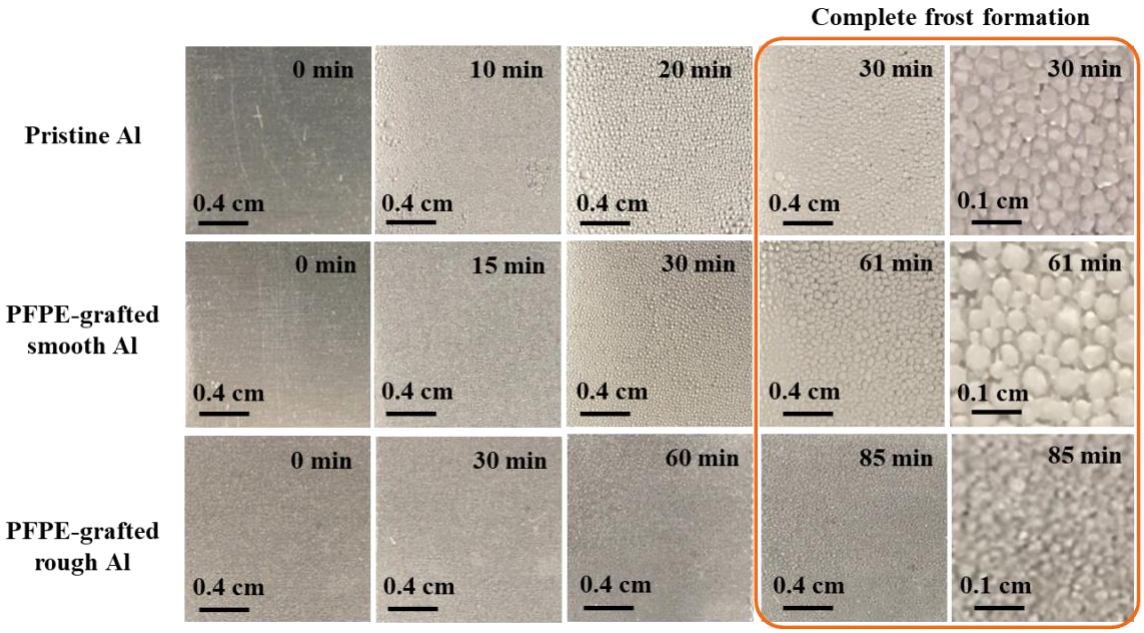

Figure 5. Time-lapse photographs showing the frost formation process on the different surfaces at a temperature of -5 ºC.

**Omniphobic capabilities of the coatings**

In addition to the anti-icing properties, the omniphobic performance was also evaluated. In particular, the repelling ability against water and olive oil was verified. Omniphobic samples and pristine aluminum were tilted to an angle of 20° and water (**Movie S1**) and olive oil (**Movie S2**) droplets were deposited on the surface. In both cases, the liquid easily rolled off of the omniphobic surface without adhesion and without leaving a trace behind. In contrast, the liquid droplets remained well adhered to the pristine aluminum under identical conditions, demonstrating the well-expressed omniphobic character of the surfaces.

## CONCLUSIONS

In summary, we have developed omniphobic aluminum surfaces by a simple 2-step method, which involves the fabrication of rough surfaces by chemical etching and further functionalization of the surface by grafting PFPE.

This unique combination of tailored hierarchical nanostructured surfaces and chemical modification allowed to obtain low SFE surfaces with outstanding omniphobic behavior, including anti-icing (freezing delay time and ice formation) and repellency of liquids. Excellent anti-icing capabilities have been proven for the optimized sample, which achieved a 20-fold delay in the water droplet freezing time, if compared to pristine aluminum, and showed the ability to repel incoming water droplets before ice nucleation occurs. Furthermore, the contact

angles demonstrated a low affinity of the substrate surface to polar and non-polar liquids, showing their potential as omniphobic surfaces.

The remarkable experimental results achieved with a low-cost and easily up-scalable process, make the reported approach a very promising solution for applications where anti-icing and repellence are required or desired.

## ASSOCIATED CONTENT

The following files are available free of charge.

Additional information regarding FESEM micrographs, 3D topographical images and surface roughness analysis of aluminum surfaces after chemical etching treatment, ATR-FTIR of PFPE deposited on rough aluminum substrates, XPS analysis of unmodified aluminum and PFPE films deposited onto smooth and rough aluminum substrates and the freezing process depiction of a water droplet is included (PDF).

Video file (Movie S1) showing the repellence ability of omniphobic surfaces against methylene blue tinted water (.MP4).

Video file (Movie S2) showing the repellence ability of omniphobic surfaces against olive oil (.MP4).

## AUTHOR INFORMATION

**Corresponding Author**

* CIDETEC, Basque Research and Technology Alliance (BRTA), Po. Miramón 196, 20014 Donostia-San Sebastián, Spain.

E-mail: jpalenzuela@cidetec.es

## Author Contributions

The manuscript was written through the contributions of all authors. All authors have given approval to the final version of the manuscript.

## Notes

The authors declare no competing financial interest.

ACKNOWLEDGMENT

This work was financially supported by the Basque Government under the ELKARTEK 2018 program contract no. KK-2018/00108 (FRONTIERS IV). I.S and M.P. acknowledge support from the University of Rijeka under the project number 18-144. M.K. acknowledges support by the Spanish Ministry of Economy and Competitiveness (MINECO) through the Maria de Maeztu Units of Excellence Programme (MDM-2016-0618).

REFERENCES

(1) Tuteja, A.; Choi, W.; Mabry, J. M.; McKinley, G. H.; Cohen, R. E. Robust Omniphobic Surfaces. *Proc. Natl. Acad. Sci. U.S.A.* **2008**, *105* (47), 18200–18205. https://doi.org/10.1073/pnas.0804872105.

(2) Hensel, R.; Neinhuis, C.; Werner, C. The Springtail Cuticle as a Blueprint for Omniphobic Surfaces. *Chemical Society Reviews* **2016**, *45* (2), 323–341. https://doi.org/10.1039/C5CS00438A.

(3) Lu, Y.; Sathasivam, S.; Song, J.; Crick, C. R.; Carmalt, C. J.; Parkin, I. P. Repellent Materials. Robust Self-Cleaning Surfaces That Function When Exposed to Either Air or Oil. *Science* **2015**, *347* (6226), 1132–1135. https://doi.org/10.1126/science.aaa0946.

(4) Ganesh, V. A.; Raut, H. K.; Nair, A. S.; Ramakrishna, S. A Review on Self-Cleaning Coatings. *J. Mater. Chem.* **2011**, *21* (41), 16304–16322. https://doi.org/10.1039/C1JM12523K.

(5) Fenero, M.; Palenzuela, J.; Azpitarte, I.; Knez, M.; Rodríguez, J.; Tena-Zaera, R. Laponite-Based Surfaces with Holistic Self-Cleaning Functionality by Combining Antistatics and Omniphobicity. *ACS Appl. Mater. Interfaces* **2017**, *9* (44), 39078–39085. https://doi.org/10.1021/acsami.7b13535.

(6) Zhang, P.; Lin, L.; Zang, D.; Guo, X.; Liu, M. Designing Bioinspired Anti-Biofouling Surfaces Based on a Superwettability Strategy. *Small* **2017**, *13* (4), 1503334. https://doi.org/10.1002/smll.201503334.

(7) Lee, J.; Boo, C.; Ryu, W.-H.; Taylor, A. D.; Elimelech, M. Development of Omniphobic Desalination Membranes Using a Charged Electrospun Nanofiber Scaffold. *ACS Appl. Mater. Interfaces* **2016**, *8* (17), 11154–11161. https://doi.org/10.1021/acsami.6b02419.

(8) Kreder, M. J.; Alvarenga, J.; Kim, P.; Aizenberg, J. Design of Anti-Icing Surfaces: Smooth, Textured or Slippery? *Nat Rev Mater* **2016**, *1* (1), 1–15. https://doi.org/10.1038/natrevmats.2015.3.

(9) Zhang, S.; Huang, J.; Cheng, Y.; Yang, H.; Chen, Z.; Lai, Y. Bioinspired Surfaces with Superwettability for Anti-Icing and Ice-Phobic Application: Concept, Mechanism, and Design. *Small* **2017**, *13* (48), 1701867. https://doi.org/10.1002/smll.201701867.

(10) Wu, X.; Chen, Z. A Mechanically Robust Transparent Coating for Anti-Icing and Self-Cleaning Applications. *J. Mater. Chem. A* **2018**, *6* (33), 16043–16052. https://doi.org/10.1039/C8TA05692G.

(11) How Do Weather Events Impact Roads? - FHWA Road Weather Management https://ops.fhwa.dot.gov/weather/q1_roadimpact.htm (accessed Apr 28, 2020).

(12) Merrill, H. M.; Feltes, J. W. Transmission Icing: A Physical Risk with a Physical Hedge. *2006 IEEE Power Engineering Society General Meeting* **2006**, 7-NaN. https://doi.org/10.1109/pes.2006.1709619.

(13) Cao, Y.; Tan, W.; Wu, Z. Aircraft Icing: An Ongoing Threat to Aviation Safety. *Aerospace Science and Technology* **2018**, *75*, 353–385. https://doi.org/10.1016/j.ast.2017.12.028.

(14) Parent, O.; Ilinca, A. Anti-Icing and de-Icing Techniques for Wind Turbines: Critical Review. *Cold Regions Science and Technology* **2011**, *65* (1), 88–96. https://doi.org/10.1016/j.coldregions.2010.01.005.

(15) Lindstrom, A. B.; Strynar, M. J.; Libelo, E. L. Polyfluorinated Compounds: Past, Present, and Future. *Environ. Sci. Technol.* **2011**, *45* (19), 7954–7961. https://doi.org/10.1021/es2011622.

(16) Buck, R. C.; Franklin, J.; Berger, U.; Conder, J. M.; Cousins, I. T.; de Voogt, P.; Jensen, A. A.; Kannan, K.; Mabury, S. A.; van Leeuwen, S. P. Perfluoroalkyl and Polyfluoroalkyl Substances in the Environment: Terminology, Classification, and Origins. *Integr Environ Assess Manag* **2011**, *7* (4), 513–541. https://doi.org/10.1002/ieam.258.

(17) Janjic, J. M.; Srinivas, M.; Kadayakkara, D. K. K.; Ahrens, E. T. Self-Delivering Nanoemulsions for Dual Fluorine-19 MRI and Fluorescence Detection. *J. Am. Chem. Soc.* **2008**, *130* (9), 2832–2841. https://doi.org/10.1021/ja077388j.

(18) Masuko, M.; Ikushima, F.; Aoki, S.; Suzuki, A. Preliminary Study on the Tribology of an Organic-Molecule-Coated Touch Panel Display Surface. *Tribology International* **2013**, *65*, 314–325. https://doi.org/10.1016/j.triboint.2013.01.019.

(19) Liu, Q.; Sun, Y.; Li, Z. Terminal Silanization of Perfluoropolyether, Polydimethylsiloxane, Their Block Polymer and the Self-Assembled Films on Plasma-Treated Silicon Surfaces. *Chem. Pap.* **2019**, *73* (1), 105–117. https://doi.org/10.1007/s11696-018-0547-y.

(20) Oldani, V.; Sergi, G.; Pirola, C.; Sacchi, B.; Bianchi, C. L. Sol-Gel Hybrid Coatings Containing Silica and a Perfluoropolyether Derivative with High Resistance and Anti-Fouling Properties in Liquid Media. *Journal of Fluorine Chemistry* **2016**, *188*, 43–49. https://doi.org/10.1016/j.jfluchem.2016.06.005.

(21) Susoff, M.; Siegmann, K.; Pfaffenroth, C.; Hirayama, M. Evaluation of Icephobic Coatings—Screening of Different Coatings and Influence of Roughness. *Applied Surface Science* **2013**, *282*, 870–879. https://doi.org/10.1016/j.apsusc.2013.06.073.

(22) Maitra, T.; Antonini, C.; Mauer, M. A. der; Stamatopoulos, C.; Tiwari, M. K.; Poulikakos, D. Hierarchically Nanotextured Surfaces Maintaining Superhydrophobicity under Severely Adverse Conditions. *Nanoscale* **2014**, *6* (15), 8710–8719. https://doi.org/10.1039/C4NR01368A.

(23) Hesse, R.; Chassé, T.; Szargan, R. Peak Shape Analysis of Core Level Photoelectron Spectra Using UNIFIT for WINDOWS. *Fresenius J Anal Chem* **1999**, *365* (1), 48–54. https://doi.org/10.1007/s002160051443.

(24) Liu, Q.; Sun, Y.; Li, Z. Terminal Silanization of Perfluoropolyether, Polydimethylsiloxane, Their Block Polymer and the Self-Assembled Films on Plasma-Treated Silicon Surfaces. *Chem. Pap.* **2019**, *73* (1), 105–117. https://doi.org/10.1007/s11696-018-0547-y.

(25) Kaynak, B.; Spoerk, M.; Shirole, A.; Ziegler, W.; Sapkota, J. Polypropylene/Cellulose Composites for Material Extrusion Additive Manufacturing. *Macromolecular Materials and Engineering* **2018**, *303* (5), 1800037. https://doi.org/10.1002/mame.201800037.

(26) Wang, D.; Oleschuk, R. D.; Horton, J. H. Surface Modification of Poly(Dimethylsiloxane) with a Perfluorinated Alkoxysilane for Selectivity toward Fluorous Tagged Peptides. *Langmuir* **2008**, *24* (3), 1080–1086. https://doi.org/10.1021/la702038t.

(27) Tada, Y.; Yoshida, H.; Miyauchi, A. Analysis on Deterioration Mechanism of Release Layer in Nanoimprint Process. *Journal of Photopolymer Science and Technology* **2007**, *20* (4), 545–548. https://doi.org/10.2494/photopolymer.20.545.

(28) Sansotera, M.; Navarrini, W.; Magagnin, L.; Bianchi, C. L.; Sanguineti, A.; Metrangolo, P.; Resnati, G. Hydrophobic Carbonaceous Materials Obtained by Covalent Bonding of Perfluorocarbon and Perfluoropolyether Chains. *J. Mater. Chem.* **2010**, *20* (39), 8607–8616. https://doi.org/10.1039/C0JM02077J.

(29) Gurav, A. B.; Guo, Q.; Tao, Y.; Mei, T.; Wang, Y.; Wang, D. Durable, Robust and Free-Standing Superhydrophobic Poly(Vinyl Alcohol-Co-Ethylene) Nanofiber Membrane. *Materials Letters* **2016**, *182*, 106–109. https://doi.org/10.1016/j.matlet.2016.06.086.

(30) Friedman, A. K.; Shi, W.; Losovyj, Y. B.; Siedle, A. R.; Baker, L. A. Mapping Microscale Chemical Heterogeneity in Nafion Membranes with X-Ray Photoelectron Spectroscopy. **2018**. https://doi.org/10.1149/2.0771811JES.

(31) Song, K.; Lee, J.; Choi, S.-O.; Kim, J. Interaction of Surface Energy Components between Solid and Liquid on Wettability, and Its Application to Textile Anti-Wetting Finish. *Polymers* **2019**, *11* (3), 498. https://doi.org/10.3390/polym11030498.

(32) Fowkes, F. M. ATTRACTIVE FORCES AT INTERFACES. *Ind. Eng. Chem.* **1964**, *56* (12), 40–52. https://doi.org/10.1021/ie50660a008.

(33) Tang, Y.; Zhang, Q.; Zhan, X.; Chen, F. Superhydrophobic and Anti-Icing Properties at Overcooled Temperature of a Fluorinated Hybrid Surface Prepared via a Sol–Gel Process. *Soft Matter* **2015**, *11* (22), 4540–4550. https://doi.org/10.1039/C5SM00674K.

(34) Rico, V. J.; López-Santos, C.; Villagrá, M.; Espinós, J. P.; de la Fuente, G. F.; Angurel, L. A.; Borrás, A.; González-Elipe, A. R. Hydrophobicity, Freezing Delay, and Morphology of Laser-Treated Aluminum Surfaces. *Langmuir* **2019**, *35* (19), 6483–6491. https://doi.org/10.1021/acs.langmuir.9b00457.

(35) Wang, L.; Teng, C.; Liu, J.; Wang, M.; Liu, G.; Kim, J. Y.; Mei, Q.; Lee, J. K.; Wang, J. Robust Anti-Icing Performance of Silicon Wafer with Hollow Micro-/Nano-Structured ZnO.

*Journal of Industrial and Engineering Chemistry* **2018**, *62*, 46–51. https://doi.org/10.1016/j.jiec.2018.01.022.

(36) Guo, P.; Zheng, Y.; Wen, M.; Song, C.; Lin, Y.; Jiang, L. Icephobic/Anti-Icing Properties of Micro/Nanostructured Surfaces. *Advanced Materials* **2012**, *24* (19), 2642–2648. https://doi.org/10.1002/adma.201104412.

(37) Fletcher, N. H. Size Effect in Heterogeneous Nucleation. *J. Chem. Phys.* **1958**, *29* (3), 572–576. https://doi.org/10.1063/1.1744540.

(38) Heydari, G.; Thormann, E.; Järn, M.; Tyrode, E.; Claesson, P. M. Hydrophobic Surfaces: Topography Effects on Wetting by Supercooled Water and Freezing Delay. *J. Phys. Chem. C* **2013**, *117* (42), 21752–21762. https://doi.org/10.1021/jp404396m.

(39) Eberle, P.; Tiwari, M. K.; Maitra, T.; Poulikakos, D. Rational Nanostructuring of Surfaces for Extraordinary Icephobicity. *Nanoscale* **2014**, *6* (9), 4874–4881. https://doi.org/10.1039/C3NR06644D.

(40) Mishchenko, L.; Hatton, B.; Bahadur, V.; Taylor, J. A.; Krupenkin, T.; Aizenberg, J. Design of Ice-Free Nanostructured Surfaces Based on Repulsion of Impacting Water Droplets. *ACS Nano* **2010**, *4* (12), 7699–7707. https://doi.org/10.1021/nn102557p.

(41) Barthwal, S.; Lim, S.-H. Rapid Fabrication of a Dual-Scale Micro-Nanostructured Superhydrophobic Aluminum Surface with Delayed Condensation and Ice Formation Properties. *Soft Matter* **2019**, *15* (39), 7945–7955. https://doi.org/10.1039/C9SM01256G.

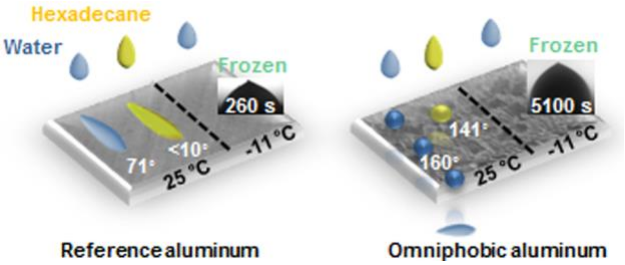
Hexadecane
Water
Frozen
260 s
71°
<10°
25 °C
-11 °C
Reference aluminum
Frozen
5100 s
141°
160°
25 °C
-11 °C
Omniphobic aluminum